JACS
JOURNAL OF THE AMERICAN CHEMICAL SOCIETY
Article
pubs.acs.org/JACS

Aqueous Self-Assembly of an Electroluminescent Double-Helical Metallopolymer

Xavier de Hatten,[†] Demet Asil,[‡] Richard H. Friend,*[,‡] and Jonathan R. Nitschke*[,†]

[†]Department of Chemistry, University of Cambridge, Lensfield Road, Cambridge CB2 1EW, U.K.
[‡]Cavendish Laboratory, University of Cambridge, JJ Thomson Avenue, Cambridge CB3 0HE, U.K.

Supporting Information

ABSTRACT: A new type of water-soluble copper-containing polymer has been synthesized using the technique of subcomponent self-assembly. Copper(I)-directed imine bond formation between triethylene glycol functionalized 1,2-phenylenediamine and 2,9-diformylphenanthroline subcomponents resulted in the formation of a chain in which two conjugated helical ligand strands wrap around a linear array of metal ions. Characterization data from a variety of analytical methods are consistent with our formulation of this material. After purification by dialysis, the polymer was shown to possess several properties of conceptual and practical interest. (1) Individual double-helical strands appear to further aggregate through entanglement of their side chains to form well-defined superstructures such as nanoscale bow ties and macrocycles, which can be imaged on a surface. (2) The material's copper(I) ions underwent reversible electrochemical oxidation in solution, whereas analogous model compounds were observed to decompose upon oxidation: the polymer's greater length appeared to stabilize oxidized states through delocalization or entrapment. (3) Photophysical measurements reveal this material to be photo- and electroluminescent. It has been successfully used for the fabrication of electroluminescent devices and shows a weak emission of white-blue light with CIE coordinates of (0.337, 0.359). This study further demonstrates the utility of the technique of subcomponent self-assembly for the straightforward generation of materials with useful properties.

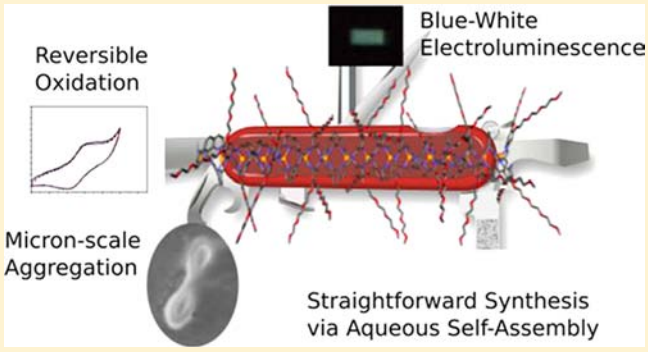

INTRODUCTION

Light-emitting electrochemical cells (LECs) are the simplest variety of electroluminescent device,[1] consisting of a thin layer of conjugated polymer sandwiched between two electrodes. The polymer layer contains an ionically conductive species that allows formation of a light-emitting p−i−n junction.[2,3] Unlike nonionic polymer light-emitting diodes, LECs do not require careful matching of electrode work functions to the band structure of the conjugated polymer,[4] allowing electrodes to be chosen from a wide range of conductive materials. Conjugated polyelectrolytes[5] can be used to construct LECs, bringing further advantages: such polymers can be easier to process, being soluble in polar solvents such as water, and their use precludes phase separation between the polymer and ion conductor during LEC operation.

The development of conjugated polyelectrolyte LECs represents a shift of complexity away from device fabrication and into the domain of chemical synthesis, allowing the deep well of synthesis knowledge to be drawn upon and applied to the creation of materials and devices that solve a clear and present problem: the generation of new, energy-efficient lighting and display technologies.

The use of chemical self-assembly as a synthetic technique can further simplify materials preparation by shifting intellectual effort away from designing molecules and toward the design of *chemical systems*[6,7] that are capable of self-assembling in such a way as to express the desired materials properties.[8−11] Here we report on the application of this concept to the preparation of a new kind of conjugated polyelectrolyte LEC.

The polymer we report herein contains complexed transition metal ions,[12] the incorporation of which is beneficial for the operation of LEDs[13−15] and LECs[16] because metal centers can augment spin−orbit coupling to allow radiative emission from the spin-triplet excitons formed by electron−hole capture, a process which has allowed devices to reach high efficiencies. Though platinum[17] and iridium[18] complexes have been used to make efficient light-emitting materials, it is desirable to avoid the use of such scarce and expensive metals; copper, as used here, has thus been investigated in emissive materials.[19−21]

Our polymer has also been designed to be water-soluble, enabling the dynamic covalent polymerization process[22] to occur under ambient conditions in water,[23] without requiring a catalyst and with no undesirable side products. The double helical polymer consists of a linear array of Cu^{I} metal ions resembling a molecular wire.[24−32]

Received: August 13, 2012
Published: October 27, 2012

dx.doi.org/10.1021/ja308055s | J. Am. Chem. Soc. 2012, 134, 19170−19178

RESULTS AND DISCUSSION

Synthesis. Compounds **A** and **B** (Scheme 1) were prepared by following a modified literature protocol.[33] Compound **C**, (4,5-bis(2-(2-(2-methoxy ethoxy)ethoxy)ethoxy)benzene-1,2-diamine), was prepared through catalytic hydrogenation of **B**.

Scheme 1. Preparation of Water-Soluble Monomer C[a]

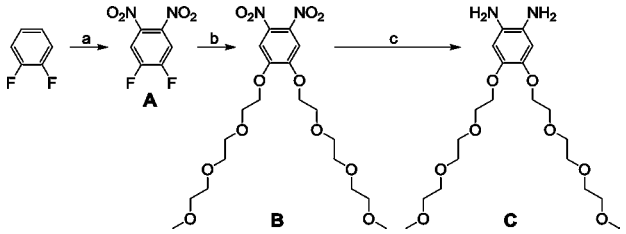

[a](a) H_2SO_4, HNO_3, 100 °C, 12 h;[33] (b) NaH, (2-(2-methoxyethoxy)-ethoxy)methanol, DME, rt, 12 h; (c) Pd/C, H_2, MeOH, rt, 12 h.

The polymerization technique chosen for this study was metal-templated imine[34,35] polycondensation. In order to validate this method in the context of double-helical metallopolymers and to provide spectroscopic points of comparison, model compounds **1** and **2** were prepared as shown in Scheme 2. We have previously reported a tetracopper helicate

Scheme 2. Preparation of Discrete Model Compounds 1 and 2 via Subcomponent Self-Assembly[a]

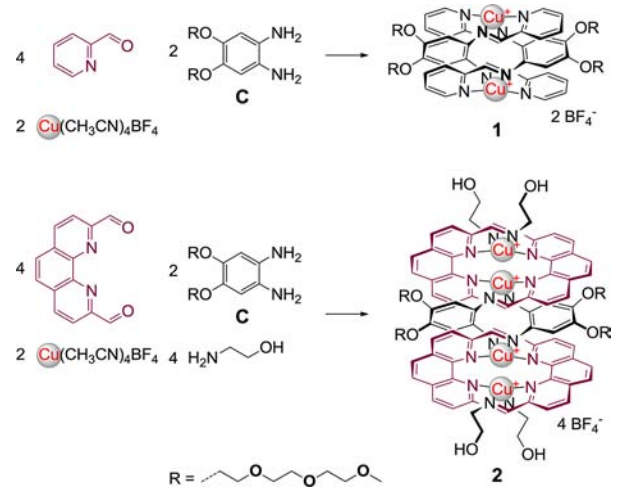

[a]D_2O or CD_3CN, 65 °C, 12 h.

structurally similar to **2**, containing four closely spaced, linearly arrayed Cu^I ions.[36] Prior studies revealed that copper-imine subcomponent self-assembly is suitable for the generation of polymers[37] including those with photoluminescent properties;[38] in order to seek new materials with useful photophysical properties, we thus sought to extend the use of subcomponent self-assembly[39] to the synthesis of double-helical water-soluble metal-containing polymers.

Polymer chain growth thus involves stepwise dynamic-covalent[40] imine bond formation between phenylene-1,2-diamine and 2,9-diformyl-1,10-phenanthroline subcomponents around copper(I) template ions. Both diamine and dialdehyde are preorganized for the formation of double-helical polymer strands as opposed to macrocycles,[41] a tendency which is reinforced by the preference of copper(I) to adopt a tetrahedral coordination geometry[42] (Figure 1).

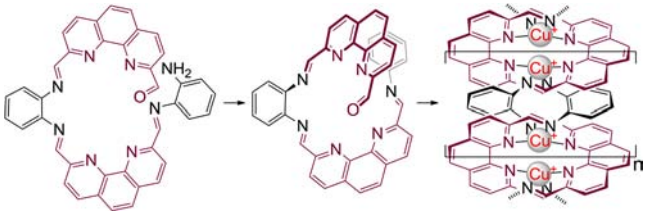

Figure 1. Mismatch between subcomponent geometries favors helical polymers over macrocycles.

In order to ensure solubility of the double-helical polymeric products, the 1,4-phenylenediamine subcomponent **C** was synthesized to incorporate two triethylene glycol chains, as shown in Scheme 1. Water-soluble diamine **C** was characterized by ^1H and ^{13}C NMR, ESI-MS, and elemental analysis (see Supporting Information).

Model compounds **1** and **2** (Scheme 2) were synthesized and characterized in order to serve as discrete spectroscopic points of reference for polymer **3** (Scheme 3). Under the same

Scheme 3. Preparation of Conjugated Metal–Organic Polymer 3[a]

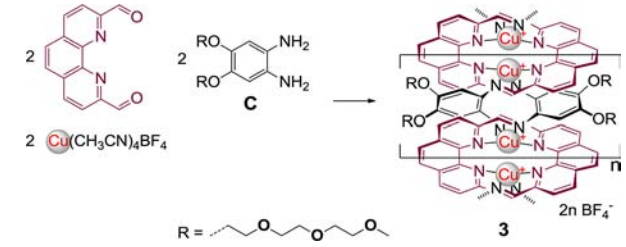

[a]Degassed D_2O, 12 h, 80 °C.

conditions and at the same concentrations used for the preparation of **3**, model compounds **1** and **2** were observed to form cleanly, suggesting that this reaction is suitable for polymer preparation. The model compounds were characterized by ^1H and ^{13}C NMR, ESI-MS, elemental analysis, cyclic voltammetry (CV), and UV–vis spectroscopy (see Supporting Information).

Polymer **3** (Scheme 3) was prepared through the aqueous reaction of equimolar amounts of 2,9-diformyl-1,10-phenanthroline and diamine **C** with copper(I).

Characterization of **3** was carried out by NMR, elemental analysis, DLS, SEM, AFM, CV, ESI-MS, UV–vis, and photoluminescence measurements, as detailed below. All results were consistent with the formation of a polymeric double helical structure.[43]

Upon formation of polymer **3**, ^1H NMR signals were observed to broaden and the end-group signals (amine and aldehyde) disappeared in contrast with spectra of model compounds **1** and **2**, which displayed well-defined NMR spectra. These spectra (Figure 2) are presented in an acetonitrile solution because the peaks of **1** and **2** are sharpest in this solvent; ^1H NMR spectra of **3** in acetonitrile (Figure 2) and water (Figure S4) are both broad over the same spectral range.

dx.doi.org/10.1021/ja308055s | J. Am. Chem. Soc. 2012, 134, 19170–19178

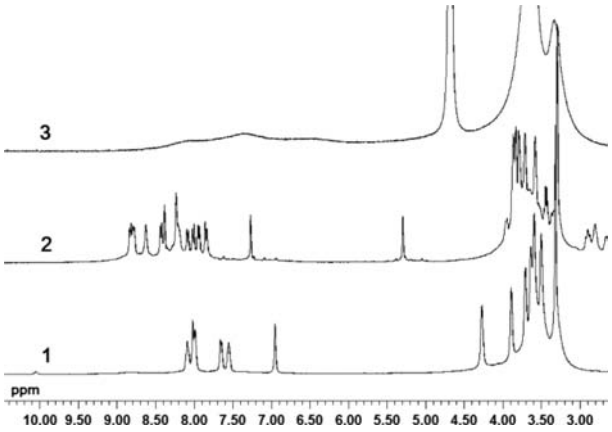

Figure 2. ^{1}H NMR spectra (CD_3CN solution) for **1**, **2**, and **3**.

The broad spectra of **3** were consistent with the formation of longer, rigid chains. The disappearance of the NMR signals from the terminal amine and aldehyde functionalities showed that they represent less than 5% of the overall signal, based upon the detection limit of the NMR, a result consistent with a polymer chain longer than 10 units on average, where each monomer unit contains two Cu^I centers (Scheme 3). After the polymerization step the mixture was purified by standard membrane dialysis against a large volume of water using SnakeSkin filtration with a membrane cutoff of 7.0 kDa, so as to remove the smaller oligomers and unreacted material. The mass removed by washing, as measured following the evaporation of the washing solution, was observed to correspond to less than 0.1 wt % of the overall mass.

Molecular Modeling. In order to visualize the three-dimensional structure of a polymer strand, molecular mechanics calculations were performed using the enhanced MM2 force field of CAChe.[44] The minimized structure of an 8-mer (containing 16 Cu atoms) is shown in Figure 3. The energy-minimized structure incorporates a linear array of copper(I) ions, and the helically twisted ligand strands do not appear more distorted than has been observed in the crystal structures of discrete analogs.[36] The modeled wire-like structure can be regarded as a linear array of Cu^I centers surrounded by a pair of helical conjugated π-systems, surrounded in turn by a sheath of electrically insulating TEG chains.

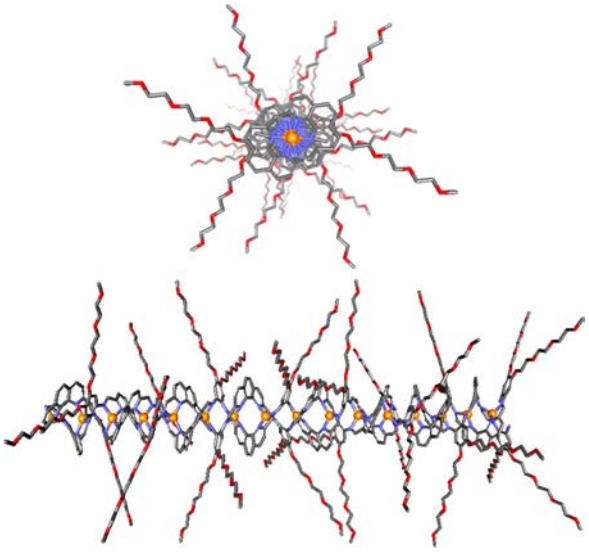

Figure 3. CAChe[44] MM2 minimized structure of a 8-mer (carbon atoms are represented in gray, oxygen in red, nitrogen in blue, and copper in orange; hydrogen atoms have been omitted for clarity).

Polymer Characterization. The size distribution of the polymer chains in solution was measured by dynamic light scattering (DLS), which has proven useful in the study of rigid-rod polyelectrolytes in water,[45] and in the dry state by SEM and AFM images (images were obtained from a spin-cast of 0.5−5 wt % solutions of the polymer mixture on a silicon surface).

Both the particle size analysis performed by DLS in solution and the SEM and AFM images, recorded on a dried layer, are consistent with two regimes of particle sizes. The smallest-diameter DLS signal (Figure 4) is assigned to the individual polymer chains. Their diameter in the Stokes−Einstein approximation ranged from 3 to 11 nm. According to the MM2 model, this corresponds to a mixture of single chains of 5 to 18 dicopper monomer units. The second signal detected by DLS, centered on 270 nm with a larger polydispersity, was assigned to larger aggregates. The intensity of this signal is consistent with the aggregates representing less than 0.05% of the total mass of the sample in solution.

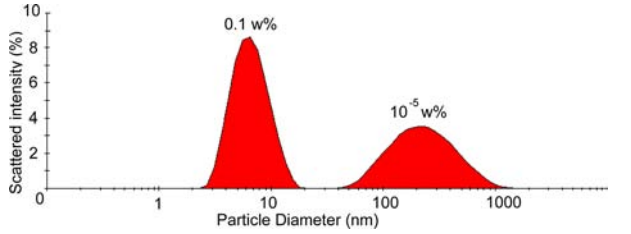

Figure 4. DLS measurement of size distribution by intensity of a 2 w% solution of purified **3** in degassed water.

Larger aggregates were also observed by AFM (Figure S5) and SEM (Figure 5). As shown in Figure 5, these micrometer-scale structures resemble bow ties or twisted loops. According to the intensity of the scattering, the concentration of aggregates is approximately 6 orders of magnitude larger on the surface layer than in solution, which indicates that the aggregation process was highly concentration dependent.

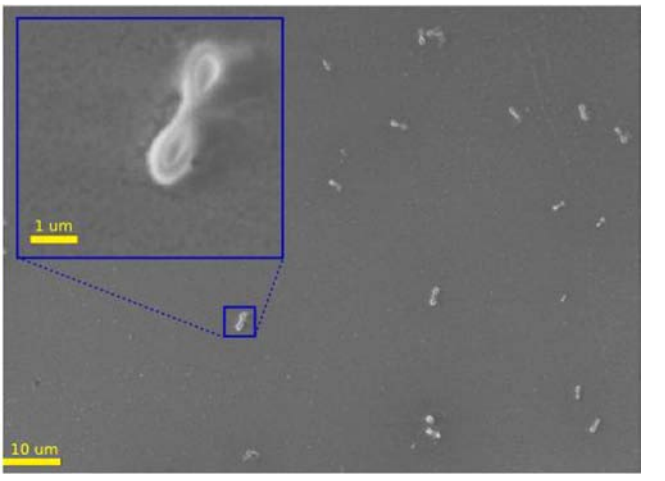

Figure 5. Scanning electron micrographs of unpurified polymer **3** spin-coated onto a silicon surface from a 1 wt % solution in water.

dx.doi.org/10.1021/ja308055s | J. Am. Chem. Soc. 2012, 134, 19170−19178

We consider the bowtie-like structures observed by SEM to be the result of nonspecific aggregations between polymer chains, possibly driven by the entanglement of the TEG side chains. Indeed, the aggregation of lipophilic structures bearing pendant ethylene glycol chains has been reported via dipole–dipole interactions on surfaces and in solution.[46−48] Our inference is supported by the observation that the concentration of aggregates in the solid state is larger than in solution by roughly 6 orders of magnitude: with fewer water molecules hydrating the side chains, the attractive interactions between oligo(ethylene glycol) moieties are expected to be enhanced. Upon dilution or addition of LiCl to the polymer solution, the apparent concentration of the aggregated structures was observed to decrease both in solution and in the solid state. In the case of dilute polymer (0.2 w%) in a 1 M LiCl solution, the aggregates were no longer observed by DLS or by surface imaging. Lithium cations are known to have a strong affinity for oligo(ethylene glycol) chains;[49,50] Coulombic repulsion between these cations is expected to prevent the polymer chains to which they are bound from interacting and aggregation.

Within aggregations, we hypothesize that individual polymer chains pack parallel to each other so as to maximize contacts between the TEG side chains. The twisted loops of Figure 5 may thus consist of circular bundles of polymer chains, in which each chain's long axis is parallel to the tangent of the cyclic loop. The relatively large radius of curvature, with respect to the length of an individual polymer chain, would allow the rigid polymer helices to avoid bending, and the crossover point at the center of the 'figure eight' would allow for further stabilizing interactions between TEG chains of parallel polymer chains from opposite sides of a circular aggregate.

UV–vis spectra were taken of **1**, **2**, and **3** in order to probe their electronic structures. These spectra are shown in Figure 6a. The UV regions (up to 380 nm) are characterized by ligand-centered (LC) bands, associated with the $\pi-\pi^*$ transitions of conjugated aromatic systems. The bands in the visible range are weaker than those in the UV; the former are assigned to metal-to-ligand charge transfer (MLCT) transitions.[51,52] The similarities between the MLCT absorption features of **2** and **3** suggest that the ground state symmetries and electronic configurations of both entities are similar. The slight difference in UV range is attributed to the extension of the aromatic π-system in **3**.

Optical band gaps were calculated by determining the low-energy absorption onset values. A band gap of 2.49 eV was measured for **1**, whereas band gaps of 2.19 and 2.14 eV were observed for **2** and **3** respectively. The closeness of the energy gap values of **2** and **3** suggest that linear extension does not greatly affect the band gap for oligo-helicates of this type, in keeping with previous theoretical predictions;[36] longer polymeric chains appear thus unlikely to display much lower band gaps than that of **3**. We posit this limited degree of decrease in band gap to be a result of the helical twisting of the polymer strands around the linear array of copper(I) template ions, which limits the degree of conjugation.

Compounds **1**, **2** and **3** exhibited weak photoluminescence (PL) in dichloromethane upon excitation into the MLCT band region (λ_{ex} = 407 nm), as shown in Figure 6b (see Figure S6 for the PL spectra in water). The emission band is broad (450–750 nm) and exhibits a λ_{max} at 557 nm for **1** and 561 nm for **2** and **3**. Upon absorption of a photon, an electron is promoted into one of the ligands, forming a photo-oxidized metal

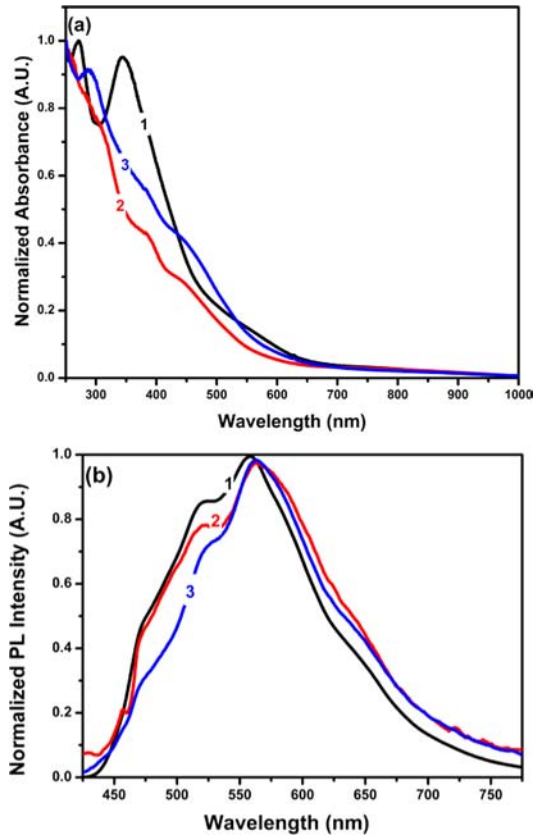

Figure 6. (a) UV–vis absorbance. (b) PL behavior of **1**, **2**, and **3** in CH_2Cl_2 (λ_{ex} = 407 nm).

center.[53] Previous work[36,54] suggests that this oxidized state is delocalized across multiple metal centers, as the proximity of the linearly arrayed copper(I) ions results in orbital overlap and a HOMO spanning multiple copper centers. The ground-state geometry of an oxidized Cu^{I}_4 helicate was calculated to be compressed along the helical axis with respect to the ground state of the nonoxidized parent.[36] In analogy to the case for bisphenanthroline Cu^{I} complexes,[52,55−57] which are known to undergo changes in ligand geometry upon MLCT excitation, we therefore infer that PL originates from the MLCT state and these compounds undergo structural changes during and following excitation, as evidenced by the large Stokes shift between absorption and PL spectra. The low PL intensity of compounds in both film and solution is attributed either to a slow radiative decay rate or to a fast nonradiative decay channel. Attempts were made to measure the radiative decay rate using time-correlated single photon counting (TCSPC), but it was found that the decay was faster than the detection limit (150 ps) of this technique.

Electrochemistry. Cyclic voltammetry (CV) studies were carried out on **1**, **2**, and **3** at room temperature in nitrogen-purged 50:50 (v/v) CH_2Cl_2/EtOH solutions. Redox processes are reported versus the Ag/AgCl gel reference electrode. None of the complexes showed a reduction couple within the solvent window; therefore only oxidation properties were studied. As shown in Figure 7, polymer **3** was observed to be the most electrochemically stable species, showing a quasi-reversible metal-centered redox process with the half-wave potential ($E_{1/2}$) at 0.52 V. The oxidation peak at 0.59 V was assigned to metal-centered oxidation, while the return peak at 0.45 V was attributed to the corresponding reduction.[58] The absence of

dx.doi.org/10.1021/ja308055s | J. Am. Chem. Soc. 2012, 134, 19170–19178

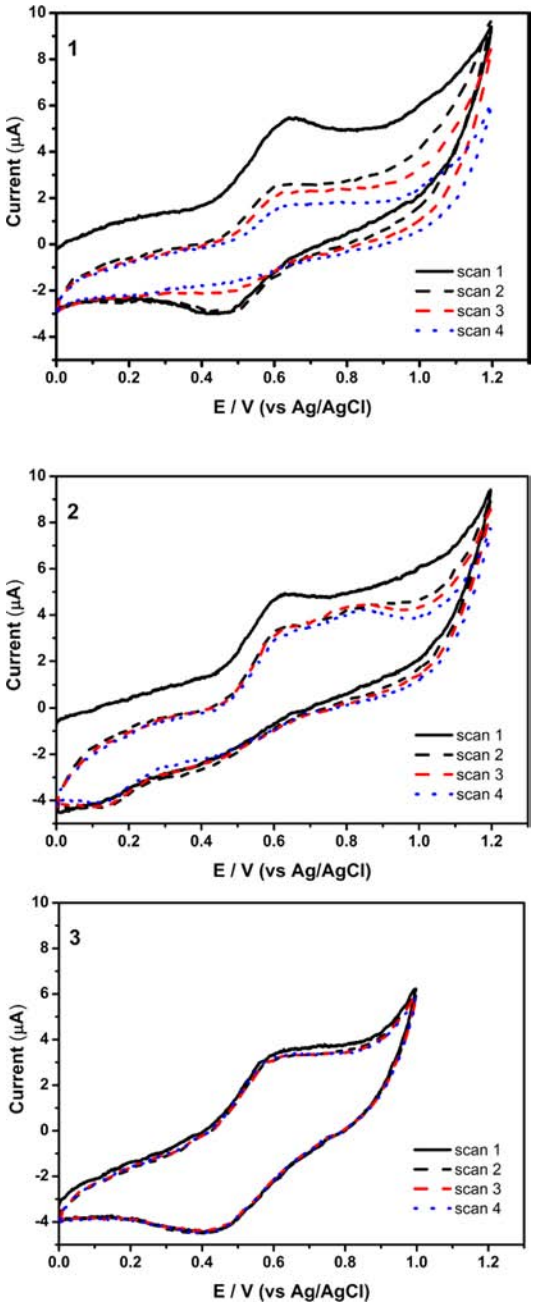

Figure 7. Cyclic voltammograms of **1**, **2**, and **3** in 0.1 M $TBAPF_6$ CH_2Cl_2/EtOH 50:50 (v/v) at 100 mV s^{-1}.

additional peaks at higher potential and the reversibility of the redox cycle suggest that the polymeric architecture of **3** lends stability against decomposition following oxidation of a portion of the copper(I) centers of the chain.

The CVs of **1** and **2**, in contrast, showed a quasi-reversible redox process with a gradual decrease of current and disappearance of the corresponding reduction peak, showing that the complex was not stable upon successive cycling. The redox process showed anodic to cathodic peak current ratios (i_a/i_c) of 1.81 and 0.76 for **1** and **3** respectively, indicating quasi-reversible systems, and peak-to-peak separations (ΔE_{pp}) of 0.15 and 0.14 V respectively. To provide a point of comparison with a reversible redox process, ferrocene$^{+/0}$ ($Fc^{+/0}$) exhibited a ΔE_{pp} of 0.502 V and i_a/i_c = 1.32 under the same experimental conditions. Complex **2** displayed an irreversible oxidation during the first oxidation cycle; the appearance of additional CV features upon cycling is consistent with chemical rearrangement and decomposition occurring following oxidation, as has been observed in related structures.[42]

The highest occupied molecular orbital (HOMO) levels were estimated with reference to the energy level of Fc and using the oxidation onset of compounds *via* eq 1:

$$E_{HOMO} = -[E_{ox-onset} + 4.8\ eV] \quad (1)$$

The HOMO level of Fc was taken as 4.8 eV below vacuum[59] and $E_{1/2}^{Fc/Fc+}$ to be 450 mV vs Ag/AgCl. The HOMO level of **3** was thus calculated to be −5.23 eV below vacuum level, and the corresponding lowest occupied molecular orbital level (LUMO) was calculated by subtracting the optical band gap (2.14 eV, as noted above) from the HOMO level obtained through CV. The LUMO level of **3** calculated by this method was −3.09 eV. As reported recently,[60] HOMO−LUMO levels estimated by this method do not give an exact value for the electron affinity but, nevertheless, help to make a comparison between different polymers and allow qualitative trends to be established.

Device Fabrication. LECs are composed of a luminescent semiconductor material in an ionic environment.[1,19] Luminescent materials studied include conjugated polymers in combination with inorganic salts and ionic transition-metal complexes (iTMCs). Due to their poor emission properties, unsubstituted bisphenanthroline Cu^I complexes have not been extensively studied to date.[61] Homoleptic substituted bisphenanthroline Cu^I complexes have attracted more attention due to their better luminescence properties, but their electroluminescence (ECL) properties have not been reported yet. Heteroleptic complexes involving bulky phosphane ligands, on the other hand, have received a great deal of attention due to their better luminescence efficiencies, and several of them have been employed in iTMC based LECs.[20,62−64] Owing to the π-acidity of the phosphane ligands, nonradiative deactivations are decreased; the MLCT excited states are found at a higher energy level compared to homoleptic bis(phenanthroline) Cu^I complexes.[65] Additionally, the excited state distortion is sterically hindered due to the bulkiness of the phosphane ligands. However, the main drawback of LECs containing heteroleptic Cu^I complexes is their short lifetime due to the chemical instability of the complexes during device operation.[20,65] Investigations of homoleptic Cu^I complexes represent an alternative approach, complementary to current avenues of investigation for new luminescent materials.

We present herein the first transition-metal-containing conjugated-polymer-based LEC (iTMP LEC). In polymer **3**, the ionic matrix was made indivisible from the main chain of the polymer, in order to speed up the diffusion of the emitting material to the electrodes and potentially improve the quantum efficiency of the LEC. The devices, as shown in Figure 8, were prepared by spin coating **3** from CH_2Cl_2 (20 mg/mL), yielding a final thickness of 100 nm on an ITO substrate, with no addition of ionic matrix. In solution and solid state, **3** was observed to be air-stable. Nevertheless, in order to prevent oxidation and contamination, the devices were fabricated in a glovebox.

The devices thus prepared showed weak electroluminescence upon applying a bias of 15 to 25 V, as depicted in Figure S7. Turn-on voltage and the luminescence were found to be dependent on the thickness of the active layer. Heteroleptic Cu^I

dx.doi.org/10.1021/ja308055s | J. Am. Chem. Soc. 2012, 134, 19170−19178

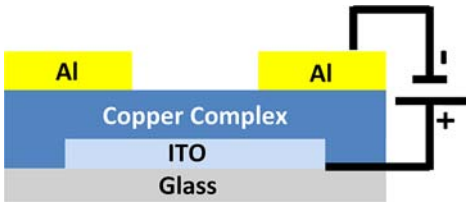

Figure 8. Device architecture on a glass substrate patterned by transparent ITO as the anode, **3** as the emissive layer, and Al as cathode.

complexes in similar device architectures have been shown to require similar turn-on voltages (18 V in ref 20 and 25 V for 40 s in ref 64). In contrast to LEDs, the emission in LECs can only occur after ionic double layers have been built up at the electrode interfaces.[66] Upon application of a constant bias, the current density and brightness of the device increase with time due to the motion and redistribution of ions. Therefore LECs do not respond to applied bias instantaneously. Response times, i.e. the time to reach the maximal brightness, are known to range from several minutes to hours.[66] It is known from extensive work on LECs based on ionic complexes of ruthenium and iridium complexes that iTMC LECs exhibit particularly long response times owing to the relatively low ion mobility.[67,68] Long response times and prebiasing were also observed for iTMC LECs employing heteroleptic Cu^{I} complexes. However in our case the device switched on within seconds of applying the bias voltage, and without any need for prebiasing.

The ECL spectrum is shown for polymer **3** in Figure 9. A broad spectrum was observed, peaking at 500 and 650 nm,

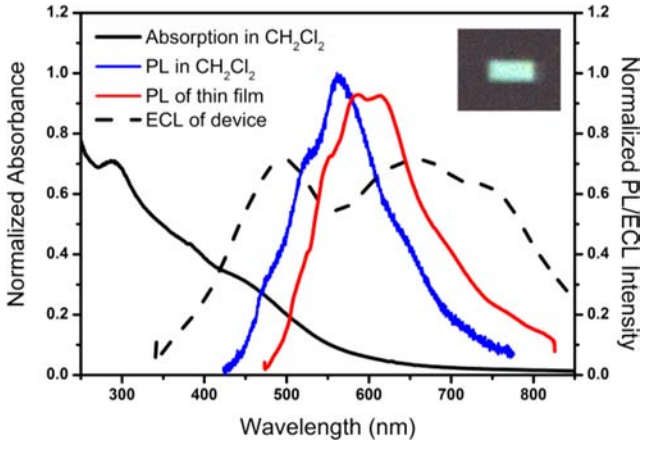

Figure 9. Absorption in CH_2Cl_2 (black), PL in CH_2Cl_2 (blue), PL of thin film (red), and ECL from the device ITO/**3** (100 nm)/Al (dashed-black) of compound **3**. Inset: picture of the white-blue light emitting pixel from the device ITO/**3** (100 nm)/Al.

which gives a white-blue color with CIE coordinates (0.337, 0.359) (see Supporting Information, Figure S8). The ECL spectrum appears shifted and broadened compared to PL spectra. The precise physical underpinnings of this phenomenon, which has been observed in other systems ranging from nanoparticles[69,70] to organic polymers,[71] are still under investigation. In the present system, the broadening and shifting of ECL may be due to the polydisperse size distribution of individual polymer chains, as reflected in DLS measurements (Figure 4), as well as the presence of different functionalities at chain ends, which may be terminated by either aldehydes or amines and which may feature two-, three-, or four-coordinate copper(I) ions or metal-free sites. Chemically different emitting centers are known to contribute to emission out of proportion to their relative abundance *via* energy transfer following excitation in an ECL device,[71] which could result in the observed broad-spectrum emission in the present case.

We believe that the emission efficiency was weak due to the following three features of the molecular structure of the polymer. First, the film morphology was not optimal, as it was observed from AFM studies that the polymer forms aggregates in acetone and water which might quench the PL through formation of interchain excited state species that relaxed nonradiatively. Second, the TEG solubilizing chains on the polymer act as insulators and hinder the mobility of holes and electrons, increasing resistivity and explaining why high voltage is required to turn the device on. Third, the double-helical shape of the polymer results in a nonplanar π-system, which in turn reduces conjugation efficiency. Efforts to mitigate these factors will be the focus of our design efforts for the next generation of iTMP LEC materials.

■ CONCLUSIONS

We have designed, synthesized, and fully characterized a multifunctional polymer using the technique of subcomponent self-assembly. The polymerization process is environmentally friendly as it occurs in water without the help of a catalyst. A simple SnakeSkin filtration from water is the only purification step required. The polymer thus obtained shows superstructure formation in the solid state and in solution *via* entanglement of its peripheral TEG chains. The polymer shows a quasi-reversible CV signal, consistent with cooperative stabilization of the partially oxidized extended metal ion chain. Promising photophysical properties were observed for the novel ionic transition metal containing a double helical polymer system, and the fabrication of the first white light emitting iTMP LEC is reported. Future work will focus upon investigation of structure−property relationships relevant to the optimization of the electrical conductivity and light-emission properties of this new class of materials.

■ EXPERIMENTAL SECTION

Reagents and solvents were purchased from Sigma-Aldrich and used without further purification unless otherwise stated. $Cu(CH_3CN)_4BF_4$[72] and 4,5-bis(2-(2-(2-methoxyethoxy)ethoxy)thoxy)-benzene-1,2-diamine were synthesized according to modified literature protocols (described below).[33,73] Polymer **3** was purified using SnakeSkin filtration with a cutoff of 3.5 or 7 kDa. DMSO-d^6 was purchased from Eurisotop and used without further purification. ^1H and ^{13}C NMR spectra were recorded on a Bruker Avance 400 or 500 spectrometer. Chemical shifts are reported in ppm downfield from the residual solvent peak for ^1H and ^{13}C, or from the methyl signal of added ^{t}BuOH (at 1.24 ppm or 70.36 ppm, respectively) in D_2O. Electronic absorbance spectra were measured in D_2O or chloroform with a Cary 100 spectrometer. Dynamic Light Scattering (DLS) measurements were recorded at 20 °C in water on a Malvern Zetasizer Nano Z. In a typical experiment 20 mg of the purified polymer were dissolved in 10 mL of degassed water. The measurements were performed at 20 °C, and 16 measurement cycles were repeated 3 times. The polydispersity obtained was 0.65. MALDI-TOF mass spectra provided by the EPSRC National MS Service Centre at Swansea were run on an Applied Biosystems 4700 Proteomics instrument; the method used was Positive Reflector Mode (PRM), the sample was scanned from 500 to 5000 m/z, and the laser intensity was set at 4230. Low-resolution electrospray ionization mass spectra (ESI-

dx.doi.org/10.1021/ja308055s | J. Am. Chem. Soc. 2012, 134, 19170−19178

MS) were obtained on a Micromass Quattro LC, infused from a Harvard Syringe Pump at a rate of 10 μL/min.

The model of **3** shown in Figure 3 was generated through energy minimization (augmented MM2 force field, 300 cycles) using the CAChe[44] software package. Atomic Force Microscopy (AFM) measurements were performed on a Dimension 2100 (Veeco Instruments, Santa Barbara, USA) in tapping mode. Phase and height images were taken at speeds of 0.5−1 lines/s using gold-coated silicon tips with spring constants of ∼20−40 N/m. Scanning Electron Microscopy (SEM) was carried out on a LEO Ultra 55 SEM with a field emission source. Accelerating voltages of 3−5 keV were used. The samples were sufficiently conducting to allow for successful imaging without requiring additional coating.

The electrochemical properties of compounds were determined by CV. Experiments were carried out in a three-electrode electrochemical cell at room temperature under N_2. A CH_2Cl_2−EtOH 50:50 (v/v) solution containing a tetrabutylammonium hexafluorophosphate ($TBAPF_6$) (0.1 M) supporting electrolyte was used as the working solution, and a Pt disk, as the working electrode. Pt wire and Ag/AgCl electrodes were used as counter and reference electrodes, respectively.

Absorption measurements, on film and in solution, were performed on a diode array Hewlett−Packard 8453 UV−vis spectrophotometer with a spectral range of 190−1100 nm and an approximately 1 nm resolution. Data were normalized, and background correction was done by a blank spectrosil. The solutions for UV−vis absorption spectroscopy were prepared by diluting solutions from stock solutions (5 mg/mL of solvent). The dilutions were 1/16, 1/10, and 1/12 in CH_2Cl_2 and 1/12, 1/10, and 1/10 in water for **1**, **2**, and **3**, respectively.

PL measurements in solution and on film were done by a pulsed 407 nm laser excitation source, a 10 MHz diode laser (PicoQuant LDH400), and the luminescence was detected using a microchannel-plate photomultiplier (Hamamatsu Photonics) coupled to a monochromator using a 500 mm spectrograph (SpectraPro2500i, Princeton Instruments) combined with a charge-coupled device (CCD) camera (PIXIS 100-F, Princeton Instruments).

Device Preparation. iTMP LECs were fabricated on indium−tin oxide (ITO) patterned glass substrates. Substrates were cleaned in an ultrasonic bath with acetone and propan-2-ol (IPA) for 15 min each, and an oxygen plasma treatment was performed for 10 min at 250 RF shortly before spin coating. The emissive layer was spin coated in the glovebox with a thickness in the range of 100 to 200 nm. The final step for device fabrication was the deposition of the top electrode and its encapsulation. An aluminum (Al; 100 nm) cathode was fabricated by thermal evaporation under vacuum (10−6 mbar) onto the device utilizing a shadow mask. The intersection of the ITO and the metal electrodes gives an active device area of 4.5 mm^2. The EL spectra were recorded using a multimode optical fiber (diameter = 600 μm) attached to an intensity-calibrated Ocean Optics USB2000 spectrometer while applying a constant voltage from a Keithley 2400 source meter.

Synthesis of 1,2-Difluoro-4,5-dinitrobenzene (A). Following a modified literature procedure,[33,73] a 500 mL two-necked round-bottom flask equipped with a reflux condenser, a large magnetic stir bar, and a Suba seal was placed in an ice bath (0 °C). **1,2-Difluorobenzene** (12.6 g, 110 mmol) was charged into the flask, followed by the careful addition of 40 mL of H_2SO_4 (95%) and 100 mL of fuming HNO_3. The resulting mixture was stirred at room temperature for another 2 h. The flask was then placed in an oil bath and slowly heated to 100 °C over a period of 2 h. The reaction mixture was then stirred at 100 °C for 12 h. The flask was subsequently cooled to room temperature, and the content was poured slowly with constant stirring over 500 mL of crushed ice. The white needle-like solid product was then collected by suction filtration and washed with 500 mL of distilled water. The white powder was then thoroughly dried under vacuum (12 h at room temperature) to yield 8.7 g (38%) of **1,2-difluoro-4,5-dinitrobenzene**. ^{1}H NMR (400 MHz, $CDCl_3$): δ = 9.18 (2H, t, J = 7.5 Hz).

Synthesis of 1,2-Bis(2-(2-(2-methoxyethoxy)ethoxy)ethoxy)-4,5-dinitrobenzene (B). Into a two-necked 250 mL round-bottom flask equipped with a large magnetic stir bar, a Suba seal, and a gas tap, **(2-(2-methoxyethoxy)ethoxy)methanol (A)** (22 mmol, 3.01 mL) was diluted in dry DME (dimethoxyethane, 100 mL). The flask was then purged with nitrogen and held under positive nitrogen pressure. NaH (60% dispersion in mineral oil) (2.5 equiv, 25 mmol, 600 mg) was added to the flask under a continuous nitrogen stream. The resulting mixture was subsequently stirred at room temperature until gas evolution stopped (approximately 1 h). **1,2-Difluoro-4,5-dinitrobenzene** (1 equiv, 10 mmol, 2.04 g) was then added in portions (over 30 min) with a continuous nitrogen stream. The flask was then closed, and the resulting slurry was stirred at room temperature overnight under a positive nitrogen pressure. The flask was then placed in an ice bath, and the reaction was quenched by slow addition of cold distilled water (1 mL). The resulting mixture was filtered through Celite, and the Celite was washed with 50 mL of dichloromethane. The solvent were subsequently removed by rotary evaporation. The residue was further purified by column chromatography on silica gel with dichloromethane/methanol (99/1 to 98/2) as the eluent. After evaporation of the solvent, **1,2-bis(2-(2-(2-methoxyethoxy)ethoxy)ethoxy)-4,5-dinitrobenzene (B)** was recovered (1.1 g, 22%). ^{1}H NMR (400 MHz, $CDCl_3$): δ = 7.46 (2H, s), 4.29 (2H, t, J = 4.7 Hz), 3.89 (4H, t, J = 4.6 Hz), 3.71 (4H, t, J = 4.8 Hz), 3.63 (8H, m), 3.52 (4H, t, J = 4.5 Hz), 3.52 (6H, s).

Synthesis of 4,5-Bis(2-(2-(2-methoxyethoxy)ethoxy)ethoxy)-benzene-1,2-diamine (C). In a round-bottom flask equipped with a large magnetic stir bar, 1,2-bis(2-(2-(2-methoxyethoxy)ethoxy)-ethoxy)-4,5-dinitrobenzene (**B**) (350 mg, 0.71 mmol) was dissolved in methanol (35 mL). A catalytic amount of 10% Pd/C (35 mg) was added to the solution. The mixture was subsequently placed under a positive pressure of hydrogen using a balloon and needle. The reaction was left to stir at room temperature overnight, resulting in the complete conversion of the nitro groups to amines. The reaction mixture was then filtered through Celite, and the Celite was washed with methanol (20 mL). The solvents were then removed by rotary evaporation to yield the pure 4,5-bis(2-(2-(2-methoxyethoxy)ethoxy)-ethoxy)benzene-1,2-diamine (**C**) as a dark green oil (Quant.). The product was used without further purification for the next step. ^{1}H NMR (400 MHz, D_2O): δ = 7.46 (2H, s), 4.29 (2H, t, J = 4.7 Hz), 3.89 (4H, t, J = 4.6 Hz), 3.71 (4H, t, J = 4.8 Hz), 3.63 (8H, m), 3.52 (4H, t, J = 4.5 Hz), 3.52 (6H, s). ^{13}C NMR (500 MHz, CD_3CN): 150.4, 145.5, 118.4, 71.5, 70.2, 70.0, 69.9, 69.3, 69.1, 57.9. ESI-MS: m/z: 433.5 ($[M + H]^+$).

Synthesis of Polymer 3. In a typical experiment the crude **4,5-bis(2-(2-(2-methoxyethoxy)ethoxy)ethoxy)benzene-1,2-diamine (C)** (320 mg 0.69 mmol) was dissolved in freshly degassed D_2O (7.0 mL) and placed in a 50 mL Schlenk flask equipped with a magnetic stir bar under a nitrogen atmosphere. To this solution, $Cu(CH_3CN)_4BF_4$ (216.6 mg, 0.69 mmol) and 2,9-diformyl-1,10-phenanthroline (162.8 mg, 0.69 mmol) were added under a continuous nitrogen stream. The resulting mixture was stirred in an oil bath at 80 °C overnight. Solvents were then removed under reduced pressure, and the residue dissolved in acetone (5 mL). The subsequent addition of pentane (50 mL) resulted in the separation of a brownish oil. Collection of the oil and subsequent removal of volatiles under reduced pressure afforded the desired polymer **3** in 81% yield. ^{1}H NMR (400 MHz, D_2O): δ = 9.0−6.0 ppm (broad aromatic signals), 4.4−2.5 ppm (broad TEG signals). No signals were observed in the ^{13}C NMR. ESI-MS: m/z: 671.74 ($[\mathbf{2Phe + 2Dia + Cu + H}]^{2+}$), 878.35 ($[\mathbf{2Phe + 3Dia + Cu + H}]^{2+}$), 931.27 ($[\mathbf{2Phe + Dia + Cu}]^{+}$), 988.38 ($[\mathbf{3Phe + 3Dia + Cu + H}]^{2+}$), 1123.42 ($[\mathbf{Phe + 2Dia + Cu}]^{+}$. Elemental analysis calcd for the polymeric species $(C_{34}H_{40}BCuF_4N_4O_8)_n \cdot 3nH_2O$: C, 48.78; H, 5.54; N, 6.67. Found: C, 48.56; H, 4.84; N, 6.74.

Synthesis of Model Compound 2. In a Schlenk flask equipped with a magnetic stir bar, freshly prepared **4,5-bis(2-(2-(2-methoxyethoxy)ethoxy)ethoxy)benzene-1,2-diamine (C)** (43.3 mg, 0.1 mmol), $Cu(CH_3CN)_4BF_4$ (62.8 mg, 0.2 mmol), 2,9-diformyl-1,10-phenanthroline (47.2 mg, 0.2 mmol), and 2-aminoethanol (12.2 mg, 12.05 μL, 0.2 mmol) were dissolved in degassed CD_3CN (2.0 mL). The flask was placed under a nitrogen atmosphere by three vacuum/nitrogen cycles. The resulting mixture was stirred in an oil bath at 65 °C overnight. The reaction was subsequently cooled to room

temperature and 20 mL of diethyl ether were added to the reaction mixture, resulting in the formation of a brown precipitate. The supernatant was decanted, and the solid was thoroughly dried under vacuum to afford **2** as a dark brown solid (86%). ^{1}H NMR (400 MHz, CD_3CN): δ = 8.82−8.73 (8H, m), 8.60 (4H, s), 8.41 (8H, d, J = 7.9 Hz), 8.36 (4H, s), 8.22−8.15 (8H, m), 8.06 (4H, d, J = 7.9 Hz), 7.99 (4H, d, J = 8.9 Hz), 7.91 (4H, d, J = 8.0 Hz), 7.82 (4H, d, J = 8.7 Hz), 7.25 (4H, s), 5.28 (4H, s), 8.36 (4H, s), 3.9−3.20 (60H, bm), 2.88 (4H, t, J = 10.2 Hz), 2.79 (4H, m), 1.53 (4H, d, J = 11.9 Hz). ^{13}C NMR (500 MHz, CD_3CN): δ = 163.2, 163.4, 153.8, 150.5, 149.0, 147.7, 142.3, 142.30, 141.5, 141.5, 138.8, 138.4, 137.6, 133.5, 132.8, 132.4, 129.3, 128.7, 127.0, 104.1, 72.6, 71.6, 71.4, 71.1, 70.1, 69.8, 66.2, 61.4, 61.0, 60.9, 58.9, 58.8, 15.5. ESI-MS: m/z: 541.23 ($[\mathbf{5}]^{4+}$), 750.63 ($[\mathbf{5} + BF_4]^{3+}$), 1168.91 ($[M + 2BF_4]^{2+}$). Elemental analysis calcd for $C_{104}H_{116}B_4Cu_4F_{16}N_{16}O_{20}\cdot 9H_2O$: C, 46.72; H, 5.05; N, 8.38. Found: C, 46.65; H, 4.66; N, 8.96.

Synthesis of the Model Compound 1. In a Schlenk flask equipped with a magnetic stir bar, freshly prepared **4,5-bis(2-(2-(2-methoxyethoxy)ethoxy)ethoxy)benzene-1,2-diamine (C)** (43.3 mg, 0.1 mmol), $Cu(CH_3CN)_4BF_4$ (31.4 mg, 0.1 mmol), and 2-formylpyridine (21.4 mg, 0.1 mmol) were dissolved in degassed CD_3CN (2.0 mL). The flask was placed under a nitrogen atmosphere by three vacuum/nitrogen cycles. The resulting mixture was stirred in an oil bath at 65 °C overnight. The reaction was subsequently cooled to room temperature and diethyl ether (20 mL) was added to the reaction mixture, resulting in the formation of a brown precipitate. The supernatant was decanted, and the solid was thoroughly dried under vacuum to afford (**1**) as a dark brown solid (73%). NMR (400 MHz, CD_3CN): δ = 8.06 (4H, t, J = 6.7 Hz), 7.99 (4H, s), 7.97 (4H, bd), 7.63 (4H, d, J = 6.8 Hz), 7.53 (4H, bt), 6.93 (4H, s), 4.24 (8H, s), 3.86 (8H, s), 3.67 (8H, s), 3.60−3.42 (24H, s), 3.29 (12H, s). ^{13}C NMR (500 MHz, CD_3CN): δ = 155.4, 150.9, 149.2, 138.9, 135.8, 129.7, 129.0, 107.6, 72.5, 71.4, 71.1, 70.9, 70.0, 69.9, 58.8. ESI-MS: m/z: 673.38 ($\mathbf{6}^{2+}$), 1435.60 ($[\mathbf{6} + BF_4]^+$). Elemental analysis calcd for $C_{64}H_{84}B_2Cu_2F_8N_8O_{16}\cdot 3H_2O$: C, 48.77; H, 5.76; N, 7.11. Found: C, 48.64; H, 5.45; N, 7.02.

■ ASSOCIATED CONTENT

Supporting Information

Experimental data, including NMR spectra, AFM, UV−vis, PL, and EL are available in the Supporting Information. This material is available free of charge via the Internet at http://pubs.acs.org.

■ AUTHOR INFORMATION

Corresponding Author

rhf10@cam.ac.uk; jrn34@cam.ac.uk

Notes

The authors declare no competing financial interest.

■ ACKNOWLEDGMENTS

This work was supported by the U.S. Army Research Office, the Marie Curie Intra-European Fellowship Scheme of the 7th EU Framework Program (X.H.), the European Research Council and the Council of Higher Education in Turkey, and Middle East Technical University (D.A.). Mass spectra were provided by the EPSRC mass spectrometry service (Swansea). We thank Rachel O'Reilly for helpful advice and Shane Heffernan for carrying out preliminary investigations into the electrical conductivity of **3**.

■ REFERENCES

(1) Costa, R. D.; Orti, E.; Bolink, H. J. *Pure Appl. Chem.* **2011**, *83*, 2115−2128.
(2) Shao, Y.; Bazan, G. C.; Heeger, A. J. *Adv. Mater.* **2007**, *19*, 365−370.
(3) Pei, Q.; Yu, G.; Zhang, C.; Yang, Y.; Heeger, A. J. *Science* **1995**, *269*, 1086−8.
(4) Edman, L. *Electrochim. Acta* **2005**, *50*, 3878−3885.
(5) Hoven, C. V.; Garcia, A.; Bazan, G. C.; Nguyen, T.-Q. *Adv. Mater.* **2008**, *20*, 3793−3810.
(6) Ludlow, R. F.; Otto, S. *Chem. Soc. Rev.* **2008**, *37*, 101−108.
(7) Nitschke, J. R. *Nature* **2009**, *462*, 736−738.
(8) Moulin, E.; Niess, F.; Maaloum, M.; Buhler, E.; Nyrkova, I.; Giuseppone, N. *Angew. Chem., Int. Ed.* **2010**, *49*, 6974−6978.
(9) Wurthner, F.; Meerholz, K. *Chem.—Eur. J.* **2010**, *16*, 9366−9373.
(10) Facchetti, A. *Angew. Chem., Int. Ed.* **2011**, *50*, 6001−6003.
(11) Orgiu, E.; Crivillers, N.; Herder, M.; Grubert, L.; Pätzel, M.; Frisch, J.; Pavlica, E.; Duong, D. T.; Bratina, G.; Salleo, A.; Koch, N.; Hecht, S.; Samorì, P. *Nat. Chem.* **2012**, *4*, 675−679.
(12) Beck, J. B.; Rowan, S. J. *J. Am. Chem. Soc.* **2003**, *125*, 13922−13923.
(13) Adachi, C.; Baldo, M. A.; Thompson, M. E.; Forrest, S. R. *J. Appl. Phys.* **2001**, *90*, 5048−5051.
(14) Lamansky, S.; Djurovich, P.; Murphy, D.; Abdel-Razzaq, F.; Lee, H.-E.; Adachi, C.; Burrows, P. E.; Forrest, S. R.; Thompson, M. E. *J. Am. Chem. Soc.* **2001**, *123*, 4304−4312.
(15) Baldo, M. A.; O'Brien, D. F.; You, Y.; Shoustikov, A.; Sibley, S.; Thompson, M. E.; Forrest, S. R. *Nature* **1998**, *395*, 151−154.
(16) Costa, R. D.; Ortí, E.; Bolink, H. J.; Monti, F.; Accorsi, G.; Armaroli, N. *Angew. Chem., Int. Ed.* **2012**, *51*, 8178−8211.
(17) Kalinowski, J.; Fattori, V.; Cocchi, M.; Williams, J. A. G. *Coord. Chem. Rev.* **2011**, *255*, 2401−2425.
(18) Coppo, P.; Plummer, E. A.; De Cola, L. *Chem. Commun.* **2004**, 1774−1775.
(19) Wang, Y.-M.; Teng, F.; Hou, Y.-B.; Xu, Z.; Wang, Y.-S.; Fu, W.-F. *Appl. Phys. Lett.* **2005**, *87*, 233512/1−233512/3.
(20) Armaroli, N.; Accorsi, G.; Holler, M.; Moudam, O.; Nierengarten, J.-F.; Zhou, Z.; Wegh, R. T.; Welter, R. *Adv. Mater.* **2006**, *18*, 1313−1316.
(21) Costa, R. D.; Tordera, D.; Orti, E.; Bolink, H. J.; Schoenle, J.; Graber, S.; Housecroft, C. E.; Constable, E. C.; Zampese, J. A. *J. Mater. Chem.* **2011**, *21*, 16108−16118.
(22) Tennyson, A. G.; Norris, B.; Bielawski, C. W. *Macromolecules* **2010**, *43*, 6923−6935.
(23) Liu, Y.; Yu, Y.; Gao, J.; Wang, Z.; Zhang, X. *Angew. Chem., Int. Ed.* **2010**, *49*, 6576−6579.
(24) Frampton, M. J.; Anderson, H. L. *Angew. Chem., Int. Ed.* **2007**, *46*, 1028−1064.
(25) Ward, M. D. *Chem. Soc. Rev.* **1995**, *24*, 121−34.
(26) Palmer, L. C.; Stupp, S. I. *Acc. Chem. Res.* **2008**, *41*, 1674−1684.
(27) Wolffs, M.; Delsuc, N.; Veldman, D.; Nguyexn, V. A.; Williams, R. M.; Meskers, S. C. J.; Janssen, R. A. J.; Huc, I.; Schenning, A. P. H. J. *J. Am. Chem. Soc.* **2009**, *131*, 4819−4829.
(28) Cacialli, F.; Wilson, J. S.; Michels, J. J.; Daniel, C.; Silva, C.; Friend, R. H.; Severin, N.; Samori, P.; Rabe, J. P.; O'Connell, M. J.; Taylor, P. N.; Anderson, H. L. *Nat. Mater.* **2002**, *1*, 160−164.
(29) Harriman, A.; Ziessel, R. *Carbon-Rich Compd.* **2006**, 26−89.
(30) Contakes, S. M.; Juda, G. A.; Langley, D. B.; Halpern-Manners, N. W.; Duff, A. P.; Dunn, A. R.; Gray, H. B.; Dooley, D. M.; Guss, J. M.; Freeman, H. C. *Proc. Natl. Acad. Sci. U.S.A.* **2005**, *102*, 13451−13456.
(31) Lipton-Duffin, J. A.; Ivasenko, O.; Perepichka, D. F.; Rosei, F. *Small* **2009**, *5*, 592−597.
(32) Terao, J.; Tanaka, Y.; Tsuda, S.; Kambe, N.; Taniguchi, M.; Kawai, T.; Saeki, A.; Seki, S. *J. Am. Chem. Soc.* **2009**, *131*, 18046−18047.
(33) Kazimierczuk, Z.; Stolarski, R.; Dudycz, L.; Shugar, D. *Nucleosides Nucleotides* **1982**, *1*, 275−87.
(34) Liu, W.; Huang, W.; Pink, M.; Lee, D. *J. Am. Chem. Soc.* **2010**, *132*, 11844−11846.
(35) Shultz, A. M.; Sarjeant, A. A.; Farha, O. K.; Hupp, J. T.; Nguyen, S. T. *J. Am. Chem. Soc.* **2011**, *133*, 13252−13255.

(36) Schultz, D.; Biaso, F.; Shahi, A. R. M.; Geoffroy, M.; Rissanen, K.; Gagliardi, L.; Cramer, C. J.; Nitschke, J. R. *Chem.—Eur. J.* **2008**, *14*, 7180−7185.
(37) Fan, J.; Saha, M. L.; Song, B.; Schonherr, H.; Schmittel, M. *J. Am. Chem. Soc.* **2012**, *134*, 150−153.
(38) de Hatten, X.; Bell, N.; Yufa, N.; Christmann, G.; Nitschke, J. R. *J. Am. Chem. Soc.* **2011**, *133*, 3158−3164.
(39) Campbell, V. E.; Nitschke, J. R. *Synlett* **2008**, *20*, 2077−3090.
(40) Rowan, S. J.; Cantrill, S. J.; Cousins, G. R. L.; Sanders, J. K. M.; Stoddart, J. F. *Angew. Chem., Int. Ed.* **2002**, *41*, 898−952.
(41) Nitschke, J. R.; Schultz, D.; Bernardinelli, G.; Gerard, D. *J. Am. Chem. Soc.* **2004**, *126*, 16538−16543.
(42) Amendola, V.; Boiocchi, M.; Brega, V.; Fabbrizzi, L.; Mosca, L. *Inorg. Chem.* **2009**, *49*, 997−1007.
(43) Liu, Y.; Wang, Z.; Zhang, X. *Chem. Soc. Rev.* **2012**, *41*, 5922−5932.
(44) CAChe. Fujitsu Limited, 2007.
(45) Liu, T.; Rulkens, R.; Wegner, G.; Chu, B. *Macromolecules* **1998**, *31*, 6119−6128.
(46) Higashihara, T.; Ohshimizu, K.; Ryo, Y.; Sakurai, T.; Takahashi, A.; Nojima, S.; Ree, M.; Ueda, M. *Polymer* **2011**, *52*, 3687−3695.
(47) Garcia, F.; Buendia, J.; Sanchez, L. *J. Org. Chem.* **2011**, *76*, 6271−6276.
(48) Bhosale, S. V.; Jani, C. H.; Lalander, C. H.; Langford, S. J.; Nerush, I.; Shapter, J. G.; Villamaina, D.; Vauthey, E. *Chem. Commun.* **2011**, *47*, 8226−8228.
(49) Tang, W.; Ogo, Y.; Minamimoto, N.; Takeoka, M. *Chem. Lett.* **2006**, *35*, 674−675.
(50) Tao, Z.; Cummings, P. T. *Mol. Simul.* **2007**, *33*, 1255−1260.
(51) Lavie-Cambot, A.; Cantuel, M.; Leydet, Y.; Jonusauskas, G.; Bassani, D. M.; McClenaghan, N. D. *Coord. Chem. Rev.* **2008**, *252*, 2572−2584.
(52) Armaroli, N.; Accorsi, G.; Cardinali, F.; Listorti, A. *Top. Curr. Chem.* **2007**, *280*, 69−115.
(53) Amendola, V.; Fabbrizzi, L.; Foti, F.; Licchelli, M.; Mangano, C.; Pallavicini, P.; Poggi, A.; Sacchi, D.; Taglietti, A. *Coord. Chem. Rev.* **2006**, *250*, 273−299.
(54) Hutin, M.; Cramer, C. J.; Gagliardi, L.; Shahi, A. R. M.; Bernardinelli, G.; Cerny, R.; Nitschke, J. R. *J. Am. Chem. Soc.* **2007**, *129*, 8774−8780.
(55) Iwamura, M.; Watanabe, H.; Ishii, K.; Takeuchi, S.; Tahara, T. *J. Am. Chem. Soc.* **2011**, *133*, 7728−7736.
(56) Iwamura, M.; Takeuchi, S.; Tahara, T. *J. Am. Chem. Soc.* **2007**, *129*, 5248−5256.
(57) Chen, L. X.; Shaw, G. B.; Novozhilova, I.; Liu, T.; Jennings, G.; Attenkofer, K.; Meyer, G. J.; Coppens, P. *J. Am. Chem. Soc.* **2003**, *125*, 7022−7034.
(58) Ruthkosky, M.; Kelly, C. A.; Castellano, F. N.; Meyer, G. J. *Coord. Chem. Rev.* **1998**, *171*, 309−322.
(59) Pommerehne, J.; Vestweber, H.; Guss, W.; Mahrt, R. F.; Baessler, H.; Porsch, M.; Daub, J. *Adv. Mater.* **1995**, *7*, 551−4.
(60) Cardona, C. M.; Li, W.; Kaifer, A. E.; Stockdale, D.; Bazan, G. C. *Adv. Mater.* **2011**, *23*, 2367−2371.
(61) Armaroli, N. *Chem. Soc. Rev.* **2001**, *30*, 113−124.
(62) Moudam, O.; Kaeser, A.; Delavaux-Nicot, B.; Duhayon, C.; Holler, M.; Accorsi, G.; Armaroli, N.; Seguy, I.; Navarro, J.; Destruel, P.; Nierengarten, J.-F. *Chem. Commun.* **2007**, 3077−3079.
(63) Zhang, Q.; Komino, T.; Huang, S.; Matsunami, S.; Goushi, K.; Adachi, C. *Adv. Funct. Mater.* **2012**, *22*, 2327−2336.
(64) Zhang, Q.; Zhou, Q.; Cheng, Y.; Wang, L.; Ma, D.; Jing, X.; Wang, F. *Adv. Funct. Mater.* **2006**, *16*, 1203−1208.
(65) Barbieri, A.; Accorsi, G.; Armaroli, N. *Chem. Commun.* **2008**, 2185−2193.
(66) Hu, T.; He, L.; Duan, L.; Qiu, Y. *J. Mater. Chem.* **2012**, *22*, 4206−4215.
(67) Buda, M.; Kalyuzhny, G.; Bard, A. J. *J. Am. Chem. Soc.* **2002**, *124*, 6090−6098.
(68) Slinker, J. D.; Rivnay, J.; Moskowitz, J. S.; Parker, J. B.; Bernhard, S.; Abruna, H. D.; Malliaras, G. G. *J. Mater. Chem.* **2007**, *17*, 2976−2988.
(69) Wang, F.; Chen, Y.-h.; Liu, C.-y.; Ma, D.-g. *Chem. Commun.* **2011**, *47*, 3502−3504.
(70) Anikeeva, P. O.; Halpert, J. E.; Bawendi, M. G.; Bulović, V. *Nano Lett.* **2007**, *7*, 2196−2200.
(71) Lu, L.-P.; Kabra, D.; Johnson, K.; Friend, R. H. *Adv. Funct. Mater.* **2012**, *22*, 144−150.
(72) Ogura, T. *Transition Met. Chem.* **1976**, *1*, 179−82.
(73) Iqbal, Z.; Hanack, M.; Ziegler, T. *Tetrahedron Lett.* **2009**, *50*, 873−875.